Inorganic Surface Nanostructuring by Atmospheric Pressure Plasma-Induced Graft Polymerization

Gregory T. Lewis, Gregory R. Nowling, Robert F. Hicks, and Yoram Cohen*

Department of Chemical and Biomolecular Engineering, University of California, Los Angeles, Los Angeles, California 90095-1592

Received February 27, 2007. In Final Form: May 29, 2007

Surface graft polymerization of 1-vinyl-2-pyrrolidone onto a silicon surface was accomplished by atmospheric pressure (AP) hydrogen plasma surface activation followed by graft polymerization in both *N*-methyl-2-pyrrolidone (NMP) and in an NMP/water solvent mixture. The formation of initiation sites was controlled by the plasma exposure period, radio frequency (rf) power, and adsorbed surface water. The surface number density of active sites was critically dependent on the presence of adsorbed surface water with a maximum observed at approximately a monolayer surface water coverage. The surface topology and morphology of the grafted polymer layer depended on the solvent mixture composition, initial monomer concentration, reaction temperature, and reaction time. Grafted polymer surfaces prepared in pure NMP resulted in a polymer feature spacing of as low as 5−10 nm (average feature diameter of about 17 nm), an rms surface roughness range of 0.18−0.72 nm, and a maximum grafted polymer layer thickness of 5.5 nm. Graft polymerization in an NMP/water solvent mixture, however, resulted in polymer feature sizes that increased up to a maximum average feature diameter of about 90 nm at [NMP] = 60% (v/v) with polymer feature spacing in the range of 10−50 nm. The surface topology of the polymer-modified silicon surfaces grafted in an NMP/water solvent mixture exhibited a bimodal feature height distribution. In constrast, graft polymerization in pure NMP resulted in a narrow feature height distribution of smaller-diameter surface features with smaller surface spacing. The results demonstrated that, with the present approach, the topology of the grafted polymer surface was tunable by adjusting the NMP/water ratio. The present surface graft polymerization method, which is carried out under AP conditions, is particularly advantageous for polymer surface structuring via radical polymerization and can, in principle, be scaled to large surfaces.

Introduction

Surface nanostructuring by grafting functional polymers to a substrate surface is a surface modification approach that has been shown to enhance the chemical functionality and alter the surface topology of native inorganic and organic materials. Surfaces modified with grafted polymers have demonstrated antifouling characteristics in separation membranes,[1−3] high chemical selectivity in chemical sensors,[4−6] and surface lubricating properties.[7,8] In such applications, the grafted polymer phase, composed of nanoscale single-molecule chains covalently and terminally bound to a substrate, serves to impart unique material properties to the substrate while maintaining the chemical and physical integrity of the native surface. Moreover, the grafted chains remain attached to the surface even when exposed to a solvent in which the polymer is completely miscible. A tethered polymer phase can be formed either by polymer grafting ("grafting to") or graft polymerization ("grafting from").[9] Surface chain coverage and spatial uniformity achieved by polymer grafting may be limited by steric hindrance. In contrast, graft polymerization, which is the focus of the present work, proceeds by sequential monomer addition, thereby allowing for the formation of a denser surface coverage.

Free radical polymerization relies on initiator species to initiate either solution polymerization, in which polymers grown in solution may bind to reactive surface sites by polymer grafting, or surface polymerization, in which monomers undergo direct surface grafting from immobilized surface initiators by graft polymerization (e.g., surface-grafted reactive groups).[9,10] However, the occurrence of competitive polymer chain grafting, chain-transfer reactions, and surface chain growth by propagation result in a polydisperse grafted polymer chain size in contrast to the more uniform surface chain size that is achieved by grafting of preformed polymer chains of a uniform size.[11] Furthermore, for inorganic substrates, the density of grafting sites for graft polymerization is limited by the availability of surface hydroxyl groups on the oxide surface that serve as the anchoring sites for surrogate surface initiators and macroinitiators. For example, the surface concentrations of hydroxyl groups on fully hydrolyzed silica and zirconia are 7.6 (4.6 molecules/nm^2) and 5.6−5.9 μmoles/m^2 (3.4−3.6 molecules/nm^2), respectively.

Plasma surface treatment, which is used for metal oxide surface etching/cleaning in microelectronics,[12,13] has been proposed in a number of recent studies as an approach to both alter surface chemistry and potentially supplant previous solution-phase initiator strategies with high-density surface activation. Early studies focused on the use of plasma treatment to modify surfaces in order to reduce the adsorption of organics and biofoulants in separation membranes,[14−16] improve surface wettability in

* Corresponding author. E-mail:yoram@ucla.edu. Tel: (310) 825-8766. Fax: (310) 206-4107.

(1) Faibish, R. S.; Cohen, Y. *J. Membr. Sci.* **2001**, *185*, 129−143.
(2) Jou, J. D.; Yoshida, W.; Cohen, Y. *J. Membr. Sci.* **1999**, *162*, 269−284.
(3) Yoshida, W.; Cohen, Y. *J. Membr. Sci.* **2004**, *229*, 27−32.
(4) Hosseini, S. H. *J. Appl. Polym. Sci.* **2006**, *101*, 3920−3926.
(5) Morohashi, H.; Nakanoya, T.; Iwata, H.; Yamauchi, T.; Tsubokawa, N. *Polym. J.* **2006**, *38*, 548−553.
(6) Abu-Lail, N. I.; Kaholek, M.; LaMattina, B.; Clark, R. L.; Zauscher, S. *Sens. Actuators, B* **2006**, *114*, 371−378.
(7) Julthongpiput, D.; Ahn, H. S.; Kim, D. I.; Tsukruk, V. V. *Tribol. Lett.* **2002**, *13*, 35−40.
(8) Drummond, C.; In, M.; Richetti, P. *Eur. Phys. J. E* **2004**, *15*, 159−165.
(9) Nguyen, V.; Yoshida, W.; Jou, J. D.; Cohen, Y. *J. Polym. Sci., Part A: Polym. Chem.* **2002**, *40*, 26−42.
(10) Chaimberg, M.; Cohen, Y. *AlChE J.* **1994**, *40*, 294−311.
(11) Yoshida, W.; Cohen, Y. *J. Membr. Sci.* **2003**, *215*, 249−264.
(12) Pearton, S. J.; Norton, D. R. *Plasma Process. Polym.* **2005**, *2*, 16−37.
(13) Cardinaud, C.; Peignon, M. C.; Tessier, P. Y. *Appl. Surf. Sci.* **2000**, *164*, 72−83.

10.1021/la700577p CCC: $37.00
Published on Web 09/08/2007

microcontact printing for poly(dimethylsiloxane) (PDMS) stamps,[17] and enhance adhesive bonding strength in advanced materials.[18,19] It was demonstrated that this versatile and environmentally benign technique had the propensity for highly efficient surface chemistry modification for both organic and inorganic materials. Plasma treatment alone, however, was shown to be an insufficient surface modification tool,[6] and it has since been noted that polymeric plasma-treated surfaces do not retain their modified chemical properties over time and with air exposure.[20] Vapor-phase plasma polymerization, in which monomer fed through plasma is initiated in the gas phase and then polymerized on a substrate surface, has also been investigated as a surface modification method.[21−23] However, surface-adsorbed radical monomer species, which are designed to polymerize with condensing monomer radicals from the vapor phase, may in fact be further modified by continuous plasma bombardment, leading to highly cross-linked, chemically and physically heterogeneous polymer films that are noncovalently adsorbed to the surface.[24−26] Also, the local concentration of monomer species in the plasma afterglow is highly dependent on the radial dimensions of the plasma source, and the resulting spatial variations in monomer deposition rate may lead to nonuniform film structure and morphology.[27]

Plasma-induced graft polymerization (PIGP) is an alternative surface modification approach in which plasma is used to activate the surface and monomer in the liquid phase is sequentially grafted to the initiation sites via free radical graft polymerization. This approach allows one to engineer a grafted polymer phase characterized by a high surface density of polymer chains that are initiated and polymerized directly from the substrate surface, thus minimizing polydisperse chain growth and improving stability under chemical, thermal, and shear stresses.[8,28,29] To date, PIGP has focused primarily on low-pressure plasma initiation and surface grafting on polymeric materials, with limited studies on inorganic oxides.[30−34] Given the complex surface chemistry and limited lifetime of reactive plasma-initiated surface species, the exact chemical nature of these plasma-generated organic moieties is yet to be established. However, various studies have inferred and quantified, through surface binding assays using radical scavengers such as 1,1-diphenyl-2-picrylhydrazyl (DPPH), the presence of surface radicals that serve as initiators for graft polymerization.[33−35] These studies have also reported that the surface radical number density that results from plasma treatment can be controlled and optimized by tuning the plasma treatment time and the radio frequency (rf) power of the plasma generator.[33−35] Yet, excessive treatment time and/or rf power results in poor surface activation, plausibly, as argued by Choi[34] and Ito,[36] because of the formation of stable inactive species.

A notable limitation for achieving PIGP on inorganic substrates, unlike polymeric materials, has been the requirement of a sufficiently dense layer of surface activation sites, created through silylation and macroinitiator grafting, that may form surface radicals for polymer initiation upon plasma treatment.[37] The surface preparation required for such techniques combined with the reliance on surface hydroxyl chemistry limits the large-scale adaptation of such methods and the level of chain density that can be achieved. Direct plasma initiation and grafting without the use of surrogate surfaces has been demonstrated qualitatively on titanium oxide particles[38] and silicone rubber materials,[39] with characteristic surface radical formation noted as a function of treatment time and rf power, similar to that for organic materials. Yet, a recent study performed by Kai et al.[40] demonstrated that, under low-pressure plasma surface treatment of Shirasu porous glass, a direct correlation between silanol density and grafted polymer density was observed. This suggests that the number density of surface radicals that may be achieved in the low-pressure plasma surface activation of inorganic oxide substrates may be limited by the native oxide surface chemistry. These findings, combined with the added requirement of ultrahigh vacuum chambers necessary for low-pressure plasma processing, indicate that the current approach is insufficient for achieving high-density surface activation and graft polymerization for large surface area modification of inorganic substrates. Although AP plasma is a promising option and has been used to alter the surface chemistry of polymeric materials,[41−43] its application to PIGP has not been demonstrated.

In the present study, an AP plasma composed of a mixture of hydrogen (1 vol %) and helium was used to activate silicon substrates directly, creating surface-bound radicals that could then initiate liquid-phase graft polymerization from these anchoring sites. The AP plasma source selected in the present study operates at a low breakdown voltage, produces a highly uniform glow discharge, and maintains low processing gas temperatures (<80 °C), which is advantageous for graft polymerization onto thermally sensitive material.[44−46] The monomer

(14) Yu, H. Y.; Hu, M. X.; Xu, Z. K.; Wang, J. L.; Wang, S. Y. *Sep. Purif. Technol.* **2005**, *45*, 8−15.
(15) Yu, H. Y.; Xie, Y.; Hu, M. X.; Wang, J. L.; Wang, S. Y.; Xu, Z. K. *J. Membr. Sci.* **2005**, *254*, 219−227.
(16) Wavhal, D. S.; Fisher, E. R. *Desalination* **2005**, *172*, 189−205.
(17) Langowski, B. A.; Uhrich, K. E. *Langmuir* **2005**, *21*, 6366−6372.
(18) Takeda, S.; Suzuki, S. *J. Vac. Sci. Technol., A* **2004**, *22*, 1297−1300.
(19) Swope, R.; Yoo, W. S.; Hsieh, J.; Shuchmann, S.; Nagy, F.; Nijenhuis, H. T.; Mordo, D. *J. Electrochem. Soc.* **1997**, *144*, 2559−2564.
(20) Steen, M. L.; Jordan, A. C.; Fisher, E. R. *J. Membr. Sci.* **2002**, *204*, 341−357.
(21) Zhang, Y.; Kang, E. T.; Neoh, K. G.; Huang, W.; Huan, A. C. H.; Zhang, H.; Lamb, R. N. *Polymer* **2002**, *43*, 7279−7288.
(22) Zhang, J.; Feng, X. F.; Xie, H. K.; Shi, Y. C.; Pu, T. S. *Acta Phys. Sin.* **2003**, *52*, 1707−1713.
(23) Zou, X. P.; Kang, E. T.; Neoh, K. G.; Zhang, Y.; Tan, K. L.; Cui, C. Q.; Lim, T. B. *Polym. Adv. Technol.* **2001**, *12*, 583−595.
(24) Choukourov, A.; Biederman, H.; Slavinska, D.; Hanley, L.; Grinevich, A.; Boldyryeva, H.; Mackova, A. *J. Phys. Chem. B* **2005**, *109*, 23086−23095.
(25) Tibbitt, J. M.; Jensen, R.; Bell, A. T.; Shen, M. *Macromol.* **1977**, *10*, 647−653.
(26) Chu, P. K.; Chen, J. Y.; Wang, L. P.; Huang, N. *Mater. Sci. Eng., R* **2002**, *36*, 143−206.
(27) Shepsis, L. V.; Pedrow, P. D.; Mahalingam, R.; Osman, M. A. *Thin Solid Films* **2001**, *385*, 11−21.
(28) Orefice, R. L.; Clark, E.; Brenna, A. B. *Macromol. Mater. Eng.* **2006**, *291*, 377−386.
(29) Bouhacina, T.; Aime, J. P.; Gauthier, S.; Michel, D.; Heroguez, V. *Phys. Rev. B: Condens. Matter* **1997**, *56*, 7694−7703.
(30) Chen, H.; Belfort, G. *J. Appl. Polym. Sci.* **1999**, *72*, 1699−1711.
(31) Chen, K. S.; Ku, Y. A.; Lin, H. R.; Yan, T. R.; Sheu, D. C.; Chen, T. M. *J. Appl. Polym. Sci.* **2006**, *100*, 803−809.
(32) Dmitriev, S. N.; Kravets, L. I.; Sleptsov, V. V.; Elinson, V. M. *Polym. Degrad. Stab.* **2005**, *90*, 374−378.
(33) Lu, W. L.; Huang, C. Y.; Roan, M. L. *Surf. Coat. Technol.* **2003**, *172*, 251−261.
(34) Choi, H. S.; Kim, Y. S.; Zhang, Y.; Tang, S.; Myung, S. W.; Shin, B. C. *Surf. Coat. Technol.* **2004**, *182*, 55−64.
(35) Suzuki, M.; Kishida, A.; Iwata, H.; Ikada, Y. *Macromolecules* **1986**, *19*, 1804−1808.
(36) Ito, Y.; Inaba, M.; Chung, D. J.; Imanishi, Y. *Macromolecules* **1992**, *25*, 7313−7316.
(37) Zhang, Y.; Tan, K. L.; Liaw, B. Y.; Liaw, D. J.; Kang, E. T.; Neoh, K. G. *Langmuir* **2001**, *17*, 2265−2274.
(38) Zhong, S. F.; Meng, Y. D.; Ou, Q. R.; Shu, X. S. *J. Appl. Polym. Sci.* **2005**, *97*, 2112−2117.
(39) Lee, S. D.; Hsiue, G. H.; Kao, C. Y. *J. Polym. Sci., Part A: Polym. Chem.* **1996**, *34*, 141−148.
(40) Kai, T.; Suma, Y.; Ono, S.; Yamaguchi, T.; Nakao, S. I. *J. Polym. Sci., Part A: Polym. Chem.* **2006**, *44*, 846−856.
(41) Hudec, I.; Jasso, M.; Cernak, M. *KGK* **2005**, *58*, 525−528.
(42) Hwang, Y. J.; Qiu, Y.; Zhang, C.; Jarrard, B.; Stedeford, R.; Tsai, J.; Park, Y. C.; McCord, M. *J. Adhes. Sci. Technol.* **2003**, *17*, 847−860.
(43) Park, S. J.; Lee, H. Y. *J. Colloid Interface Sci.* **2005**, *285*, 267−272.
(44) Moravej, M.; Yang, X.; Nowling, G. R.; Chang, J. P.; Hicks, R. F.; Babayan, S. E. *J. Appl. Phys.* **2004**, *96*, 7011−7017.
(45) Park, J.; Henins, I.; Herrmann, H. W.; Selwyn, G. S.; Jeong, J. Y.; Hicks, R. F.; Shim, D.; Chang, C. S. *Appl. Phys. Lett.* **2000**, *76*, 288−290.

chosen for this study, 1-vinyl-2-pyrrolidone (VP), is of interest because poly(vinyl pyrrolidone) has excellent biocompatible properties,[31] has been proposed as a surface modifier to reduce membrane fouling,[30] and is miscible in both aqueous and organic media.[9,30,31] Experimental results are reported for both plasma surface initiation and VP graft polymerization, focusing on controlling and optimizing surface initiator density and the impact of surface graft polymerization conditions on the resulting surface topology of the terminally anchored polymer surface layer.

Materials and Methods

Materials. Prime-grade silicon ⟨100⟩ wafers used in this study were obtained from Wafernet, Inc. (San Jose, CA). Native wafer samples were single-side polished and cut to 1 × 1 cm^2 pieces for processing. Deionized (DI) water was produced using a Millipore (Bedford, MA) Milli-Q filtration system. Hydrofluoric acid, sulfuric acid, aqueous hydrogen peroxide (30%), and technical-grade hydrochloric acid were purchased from Fisher Scientific (Tustin, CA). Anhydrous *N*-methyl-2-pyrrolidone (99.5%), reagent-grade toluene, and tetrahydrofuran were obtained from Fisher Scientific (Tustin, CA). 1-Vinyl-2-pyrrolidone (99%) with sodium hydroxide inhibitor (<0.1%) was used as received and was obtained from Alfa Aesar (Ward Hill, MA). Aqueous ammonium hydroxide (50%) was purchased from LabChem, Inc. (Pittsburgh, PA). Surface radical determination was accomplished using the 2,2,6,6-tetramethyl-1-piperidinyloxy radical (TEMPO, 98%), which was obtained from Sigma-Aldrich (St. Louis, MO).

Substrate Cleaning and Conditioning. Silicon substrates were subjected to a multistep surface cleaning and conditioning process to remove surface contaminants and the native oxide layer on as-received wafers. Substrates were cleaned in piranha solution (3:1 sulfuric acid/hydrogen peroxide) for 10 min at 90 °C and then triply rinsed to remove residuals. Substrates were then dipped in a 20% (v/v) aqueous solution of hydrofluoric acid to remove the native oxide layer and then triply rinsed as before. The silicon substrates were immersed in 1% (v/v) aqueous hydrochloric acid at ambient temperature for 8 h and then placed in DI water for 1 h to hydrolyze the silicon surface fully. Hydrolyzed silicon wafers were then oven dried under vacuum at 100 °C for 10 h to remove surface water.

Prior to surface activation by plasma treatment, the dried silicon substrates were conditioned in a humidity chamber to adjust the level of adsorbed surface water. The insulated chamber was designed for control over both temperature (±2 °C) and humidity (±5%) and was humidified with DI water over the range of 20−70% relative humidity (RH) at 22 °C. Silicon substrates were allowed to equilibrate for at least 12 h prior to plasma surface treatment.

Surface Initiator Determination. The presence and relative abundance of surface radicals that are formed during plasma treatment were determined using 2,2,6,6-tetramethyl-1-piperidinyloxy (TEMPO), which is a well-known free radical scavenger that covalently bonds to silicon surface radicals.[47,48] The presence of surface-bound TEMPO (as detected by FTIR) served as an indirect measure of the density of surface radicals. Silicon substrates (1 × 1 cm^2) were plasma treated and immediately immersed in a solution of 0.1 mM TEMPO dissolved in *N*-methyl-2-pyrrolidone and allowed to react over a 24 h period at 90 °C. The substrates were then removed and sonicated in tetrahydrofuran for 2 h to remove surface-adsorbed TEMPO and finally oven dried under vacuum at 100 °C overnight to remove residual solvent. Grazing angle FTIR spectroscopy was used to detect the surface-bound TEMPO by collecting spectra from at least three locations for each wafer. The presence of TEMPO was confirmed by FTIR absorption peaks at 3019 and 1100 cm^{-1} for aromatic carbon atoms and nitroxide functional groups, respectively. The absorbance spectrum was compared with the solution concentration

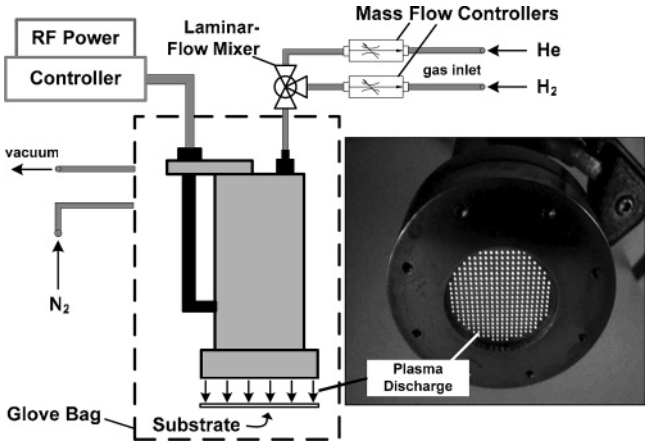

Figure 1. Schematic of atmospheric pressure plasma source process configuration with an image (inset) of the plasma source discharge region (diameter = 3.25 cm).

to develop the linear calibration curve between concentration and absorbance over the initial TEMPO concentration range of 1.0−0.001 mM.

Plasma Surface Activation and Graft Polymerization. Silicon substrates were plasma treated in a glove bag under an inert nitrogen atmosphere to prevent exposure to oxygen, which destroys surface free radicals. The AP plasma source used in the present study was designed as a cylindrical plasma jet (Figure 1) for which a detailed description is provided elsewhere.[46] The process is configured for remote AP plasma surface treatment, with the substrate positioned no less than 1 cm from the exit region, to reduce ion bombardment of the surface. The AP plasma source was operated at 100−250 V and was driven by rf power at 13.56 MHz. A mixture of 1% by vol ultrahigh purity hydrogen (99.999%) in helium (99.999%) was delivered to the AP plasma source at a total flow rate of 30.4 L/min, and the surface was exposed to plasma for a period of 5−50 s at an rf power of 20−60 W. Following plasma treatment, the silicon substrates were immediately immersed in DI water to stabilize the surface radical and then transferred into a degassed monomer/solvent solution with initial monomer concentrations in the range of 10−50% (v/v) 1-vinyl-2-pyrrolidone in (1) DI water, (2) *N*-methyl-2-pyrrolidone, or (3) a combination of the above two solvents. Unless otherwise noted, the concentration of the initial monomer and solvent in solution was measured by % (v/v). The pH for aqueous polymerization reaction mixtures was adjusted with ammonium hydroxide to reduce side reactions.[28] The temperature of the reaction mixture was maintained at 80 ± 1 °C, and each reaction was allowed to proceed for a period of at least 8 h. At the termination of the graft polymerization reaction, the surface-modified silicon substrates were triply rinsed in DI water and then sonicated for 2 h to remove potentially adsorbed homopolymer. Cleaned substrates were then oven dried overnight under vacuum at 100 °C.

Surface Characterization. Surface analysis by Fourier transform infrared (FTIR) spectroscopy was carried out by using a Bio-Rad FTS-40 with a grazing angle attachment (Varian Digilab Division, Cambridge, MA). Grazing angle IR spectra for TEMPO-reacted and plasma-treated surfaces were processed by subtraction from the spectra for clean, native silicon substrates. The resulting spectra were represented in Kubelka−Munk units, which have absorbance values that are proportional to the surface species concentration.

Contact angle measurements for the poly(vinyl pyrrolidone)-grafted silicon wafers were obtained by the sessile-drop method with a Kruss model G-23 contact angle instrument (Hamburg, Germany). Before the measurements, each wafer was rinsed and sonicated separately in tetrahydrofuran and then DI water, each for 15 min. The wafer was subsequently oven dried under vacuum for 30 min at 80 °C. Measurements were made using DI water at 40−50% relative humidity and 22 °C. Each contact angle datum was obtained by averaging the results from five separate drops on different areas of a given surface. The size and volume of the drops were kept

(46) Schutze, A.; Jeong, J. Y.; Babayan, S. E.; Park, J.; Selwyn, G. S.; Hicks, R. F. *IEEE Trans. Plasma Sci.* **1998**, *26*, 1685−1694.
(47) Pitters, J. L.; Piva, P. G.; Tong, X.; Wolkow, R. A. *Nano Lett.* **2003**, *3*, 1431−1435.
(48) Guisinger, N. P.; Basu, R.; Baluch, A. S.; Hersam, M. C. *Ann. N.Y. Acad. Sci.* **2003**, *1006*, 227−234.

approximately constant to reduce variations in contact angle measurements.

The film thickness of the plasma-treated surface and the polymer-grafted substrates was determined using a Sopra GES5 spectroscopic ellipsometer (SE) (Westford, MA). The broadband variable-angle SE was operated over a range of 250−850 nm, and the ellipsometric data that were collected were fitted to user-defined multilayer film models with the film thickness calculated through the use of the Levenberg−Marquardt regression method. Each measurement was averaged over five locations on the substrate, and the standard deviation did not exceed ±10%.

Atomic force microscopy (AFM) imaging was performed using a Multimode AFM with a Nanoscope IIIa SPM controller (Digital Instruments, Santa Barbara, CA). All AFM scans were conducted in tapping mode in ambient air using NSC15 silicon nitride probes (Digital Instruments, Veeco Metrology Group, Santa Barbara, CA) with a force constant between 20 and 70 N/m, a nominal radius of curvature of 5−10 nm, and a side angle of 20°. AFM scans (1 × 1 μm^2) on silicon substrates were taken at a scan rate of 0.5−1 Hz. At least five locations were sampled for each modified substrate, with two scans taken for each location. Surfaces were imaged at 0 and 90° to ensure that images were free of directional errors. Height data and phase data were taken simultaneously for the same scan area. The root-mean-square (rms) surface roughness was determined directly from height data for 1 × 1 μm^2 scans where R_{rms} is the rms roughness, Z_i is the ith height sample out of N total samples, and Z_{av} is the mean height.

$$R_{rms} = \sqrt{\frac{\sum (Z_i - Z_{av})^2}{N}} \quad (1)$$

The skewness, S_{skew}, which is a measure of the asymmetry of the height distribution data about the mean, was determined from

$$S_{skew} = \frac{\sum (Z_i - Z_{av})^3}{(N-1)\sigma^3} \quad (2)$$

where σ is the standard deviation. The polymer volume for the graft polymerized surfaces was determined over a 1 × 1 μm^2 area by volume integration over the grafted polymer area with respect to the z-height profile of the polymer surface features. To minimize the contribution of native silicon wafer features to the polymer volume, the average z height of the native silicon surface (0.5−1.0 nm), determined from five locations for each surface, was subtracted from the surface feature height data when integrating to obtain the total polymer volume. To determine the height distributions of the modified surfaces, the z-height data used for polymer volume measurements was compared to a Gaussian distribution in order to clarify the presence of tails (small or large features) in the distribution. Feature spacing and average feature diameter were determined by measurements taken from 10 different locations over a 1 × 1 μm^2 area, whereby feature boundaries were defined on the basis of digital image pixel analysis.

Results and Discussion

The present approach to AP plasma-induced graft polymerization (PIGP) of inorganic silicon, as illustrated in Figure 2, consisted of a multistep process involving (1) surface cleaning, (2) surface conditioning, (3) plasma surface initiation (treatment), and (4) graft polymerization. Native oxide films present on inorganic silicon are heterogeneous in nature, can easily be etched in basic media, and therefore were removed first to ensure effective graft polymerization. The substrate was then conditioned in a humidity chamber to create a thin layer of adsorbed surface water and then exposed to AP plasma to generate surface initiation sites. Consistent with previous studies on plasma activation of polymeric substrates, the resulting surface density of surface initiation sites was, in part, determined by the plasma treatment

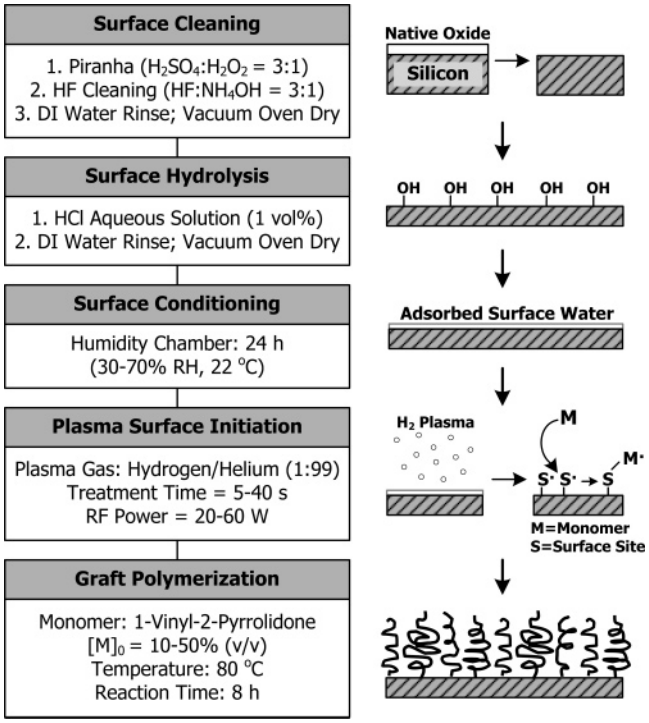

Figure 2. Illustration of multistep process plasma-induced graft polymerization.

time and the rf power.[33−35] However, in the present study, it was found that, unlike the situation for polymeric surfaces, control of the adsorbed surface water coverage was essential in order to achieve a reasonable level of surface activation on the inorganic substrates so as to obtain a dense grafted polymer layer. The combined effect of plasma surface treatment and adsorbed surface water on the generation of surface initiation sites was investigated using a TEMPO binding assay as discussed later.

Plasma Surface Activation. Hydrogen plasma, which is commonly used in nanoelectronics for surface cleaning, is composed of hydrogen atoms formed by electron impact dissociation that may either recombine further downstream from the discharge region or can be used for surface treatment.[49] Hydrogen plasma was chosen in the current study because of its intrinsic low silicon etch rate[50,51] and because it can be operated at low processing temperatures, unlike oxygen plasma, which requires a high power density for processing. For example, the plasma gas temperature in the present study did not exceed 100 °C over an exposure period of 60 s at an rf power of 60 W. Therefore, one would expect that surface activation would not be due to high-temperature surface treatment but instead would be the result of plasma−surface interactions. This assertion is supported by quantum chemical simulations of hydrogen plasma treatment of a silicon surface, performed by Ishii et al.,[52] that suggested that hydrogen plasma species have sufficient energy to break Si−Si bonds, creating silicon dangling bonds (i.e., silicon radicals) both on the surface and within the subsurface. However, prolonged exposure of the substrate to plasma may result in surface etching and physical degradation of the surface. Surface etching of silicon using a low-pressure hydrogen plasma has been shown to increase with decreasing substrate temperature,

(49) Moravej, M.; Babayan, S. E.; Nowling, G. R.; Iang, X.; Hicks, R. F. *Plasma Sources Sci. Technol.* **2004**, *13*, 8−14.
(50) Choi, K.; Ghosh, S.; Lim, J.; Lee, C. M. *Appl. Surf. Sci.* **2003**, *206*, 355−364.
(51) Hwang, K. H.; Yoon, E. J.; Whang, K. W.; Lee, J. Y. *J. Electrochem. Soc.* **1997**, *144*, 335−339.
(52) Lu, F.; Corbett, J. W.; Snyder, C. *Phys. Lett. A* **1988**, *133*, 249−252.

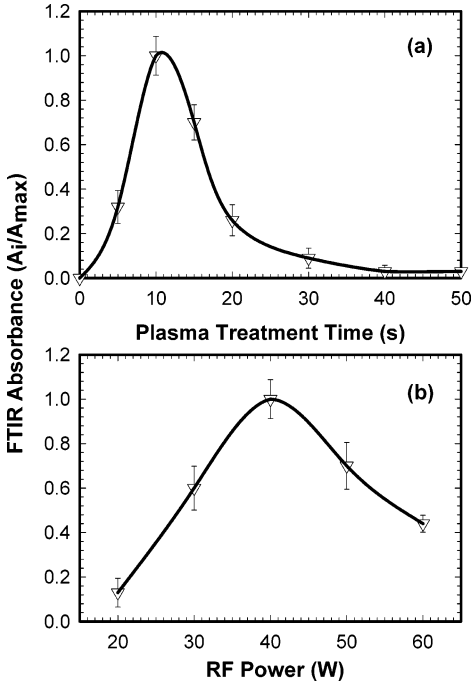

Figure 3. Effect of (a) plasma treatment time (rf power = 40 W) and (b) rf power (treatment time = 10 s) on the presence of surface radicals (detected by TEMPO binding assay) formed by atmospheric pressure plasma surface treatment (RH = 50% at 22 °C for both a and b).

approaching a maximum of 6.0 nm/min at a substrate temperature of 25 °C.[53] It was also reported that conelike projections of 100−200 nm diameter appeared when the substrate temperature was raised to 200 °C. This behavior was attributed to hydrogen diffusion into the subsurface and vaporization and redeposition of silicon hydrides.[54] However, it is important to note that, in the current system, AP plasma surface treatment resulted in less than a 0.5 Å increase in rms roughness from R_{rms} = 0.17−0.21 nm over the longest treatment period of 120 s at an rf power of 40 W. Moreover, AFM images did not reveal any evidence of pitting or anisotropic etching over a 1 × 1 μm^2 surface area.

The presence of surface radical species generated by AP hydrogen plasma surface treatment was verified using the TEMPO binding assay. The impacts of both plasma treatment time and rf power were first evaluated to select the optimal plasma treatment conditions. The surface density of radical species, as suggested by the TEMPO surface-binding analysis, increased with plasma exposure times according to a power law dependence as illustrated in Figure 3a up to a maximum coverage that was reached at 10 s treatment time (rf power of 40 W). Extending the plasma treatment time beyond 10 s resulted in a similar decline in radical surface coverage by more than 70 and 90% for 20 and 30 s exposure periods, respectively. These findings are in general agreement with other studies performed on organic materials in which an optimal plasma exposure treatment time was found that maximized the surface radical density.[33−35] This behavior is due to surface radical formation and subsequent passivation, leading to the removal or inactivation of surface initiators as the residence time of hydrogen plasma species is increased at the surface. However, it should be noted that the treatment time interval necessary for optimal surface radical formation using low-pressure activation of polymeric materials was reported to

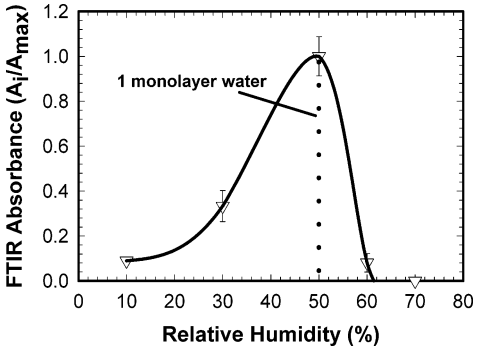

Figure 4. Effect of absorbed surface water coverage on the presence of surface radicals (detected by TEMPO binding assay) formed by atmospheric pressure plasma surface treatment (treatment time = 10 s; rf power = 40 W).

be significantly longer than for AP plasma treatment of inorganic surfaces: 180 s for argon plasma treatment of polyethylene,[33] 60 s for argon plasma treatment of poly(acrylic acid),[39] and 30 s for oxygen plasma treatment of polyurethane.[34] Plasma power had a qualitatively similar effect to treatment time on the formation and surface coverage of radical initiator sites as shown in Figure 3b. The site density of surface radicals increased with rf plasma power to a maximum reached at an rf power of 40 W (treatment time of 10 s) and then decreased slowly with further increases in rf power. In plasma processing, an increase in plasma power leads to increased electron−atom collisions in the gas phase, generating a higher density of reactive species in the plasma gas and therefore at the substrate surface.[55] Thus, similar to the impact of increased plasma treatment time, radicals that were created on the surface were subsequently passivated by overexposure to plasma species.

Consideration of the surface chemistry involved in the stabilization of surface radicals on inorganic substrates led to strategies that improved the surface radical number density. Whereas the chemical surface properties of polymeric surfaces allow for the formation of pseudostable initiation sites[56] (e.g., epoxides) upon plasma treatment, inorganic surface radicals are unstable and undergo molecular rearrangements such as atomic recombination and/or decomposition to form nonradical dormant species.[57] To maintain surface activity (for subsequent graft polymerization) for a sufficiently long period of time, it was found in the present study that adsorbed surface water was critical in the formation and stabilization of inorganic surface radicals. It is postulated that the beneficial role of adsorbed surface water may be the result of the reaction of surface radicals with water to form surface peroxides or may possibly be due to the stabilization of the silicon radical through hydrogen bonding with water. Accordingly, the impact of surface water on the creation of surface initiation sites was evaluated in a series of experiments in which the degree of surface water coverage was varied by equilibrating the substrate in a humidity-controlled chamber. As shown in Figure 4, the density of surface radicals, as implied by the TEMPO binding analysis, increased with increasing adsorbed surface water coverage up to a maximum at 50% relative humidity (% RH) at 22 °C (for the optimal plasma exposure of 10 s at an rf power of 40 W). As previously noted by Collins et al.,[58] for fully hydroxylated silica surfaces with a

(53) Strass, A.; Hansch, W.; Bieringer, P.; Neubecker, A.; Kaesen, F.; Fischer, A.; Eisele, I. *Surf. Coat. Technol.* **1997**, *97*, 158−162.

(54) Huang, Y. L.; Ma, Y.; Job, R.; Scherff, M.; Fahrner, W. R.; Shi, H. G.; Xue, D. S.; David, M. L. *J. Electrochem. Soc.* **2005**, *152*, C600−C604.

(55) Jeong, J. Y.; Park, J.; Henins, I.; Babayan, S. E.; Tu, V. J.; Selwyn, G. S.; Ding, G.; Hicks, R. F. *J. Phys. Chem. A* **2000**, *104*, 8027−8032.

(56) Andreozzi, L.; Castelvetro, V.; Ciardelli, G.; Corsi, L.; Faetti, M.; Fatarella, E.; Zulli, F. *J. Colloid Interface Sci.* **2005**, *289*, 455−465.

(57) Passari, L.; Susi, E. *J. Appl. Phys.* **1983**, *54*, 3935−3937.

(58) Collins, K. E.; de Camargo, V. R.; Dimiras, A. B.; Menezes, D. T. C.; da Silva, P. A.; Collins, C. H. *J. Colloid Interface Sci.* **2005**, *291*, 353−360.

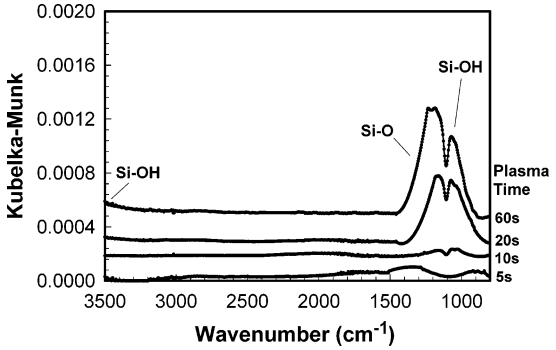

Figure 5. Grazing angle FTIR spectra of hydrogen plasma-treated silicon for treatment periods of 5, 10, 20, and 60 s (rf power = 40 W; RH = 50% at 22 °C).

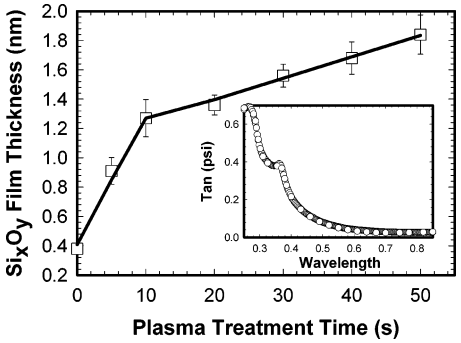

Figure 6. Growth of thin silicon oxide Si_xO_y film as a function of plasma treatment time at rf power = 40 W and RH = 50% at 22 °C. (Inset) Curve fitting of the film model with Levenberg−Marquardt regression.

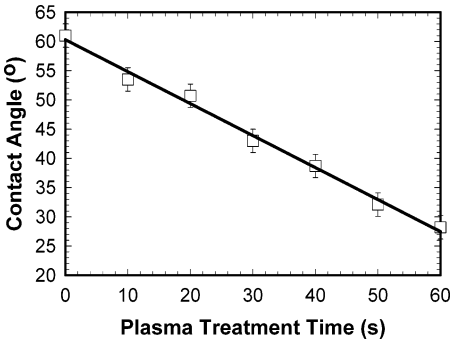

Figure 7. Effect of plasma treatment time on water contact angle for silicon substrates (rf power = 40 W; RH = 50% at 22 °C).

silanol concentration of 7.6 μmoles/m^2, the formation of a single adsorbed monolayer of water occurs at about 51% RH at 22 °C, assuming a 1:1 surface water/silanol ratio. Thus, it may be inferred that the maximum density of surface-active sites obtained in the present study at 50% RH corresponded to approximately a single monolayer coverage of surface water. At surface water coverage above a monolayer (i.e., >50% RH), a significant decrease of 90% in surface radical density occurred as the relative humidity increased from 50 to 60%. It is noted that the atomic radius of a hydrogen plasma species is approximately 0.5 Å and the film thicknesses of adsorbed surface water for one, two, and three monolayers are 1.2, 2.7, and 4.3 Å, respectively.[59] Therefore, it is plausible that as the surface water layer thickness increases the water film becomes a physical barrier to plasma particles, thereby reducing direct interactions with the underlying surface. The above results illustrate that optimal control of surface water coverage on inorganic substrates, along with plasma treatment time and rf power, was essential to controlling the density of surface initiation sites necessary for graft polymerization.

Surface activation and the impact of surface passivation, due to overexposure of the substrate, can be inferred from FTIR spectra of the plasma-treated surface shown in Figure 5. At short exposure times of 5 and 10 s, low-intensity absorption peaks associated with Si−O−Si and Si−OH bond stretching at 1150 and 1060 cm^{-1}, respectively, were apparent. However, the peak intensities for these groups increased as the plasma treatment time was increased. At longer exposure times, the Si−O−Si and Si−OH peak height ratios (A_{1150} cm^{-1}/A_{1060} cm^{-1}) increased from ratios of 1.1:1 to 1.6:1 with increasing treatment times from 20 to 60 s, respectively. The above results are consistent with the assertion that at longer treatment times not only is the surface passivated but, as suggested in previous studies, hydrogen atoms diffuse into the subsurface to create silicon dangling bonds (i.e., silicon radicals).[52,54] Silicon radicals that are created may then react with water to form a thin film composed of Si_xO_y moieties interspersed within the crystalline silicon. Quantification of the growth of these Si_xO_y thin films was obtained from ellipsometric film thickness measurements as a function of plasma treatment time as shown in Figure 6 (rf power of 40 W and surface conditioning of 50% RH at 22 °C). Prior to plasma treatment, the silanol film thickness, generated during surface hydrolysis, was measured to be about 0.4 nm. For a short plasma treatment exposure period (<10 s), growth of the thin, subsurface Si_xO_y film increased with exposure time, attaining a thickness of about 1.3 nm over a treatment time of 10 s corresponding to an initial growth rate of 0.1 nm/s. For plasma exposure periods greater than 10 s, there was an order of magnitude decrease in the Si_xO_y film growth rate to 0.01 nm/s. This decrease in growth rate is likely to be the result of surface passivation of activated surface sites and/or mass transfer limitations associated with the diffusion or penetration of hydrogen plasma into the highly dense subsurface. From the above results that demonstrate the incorporation of oxygen into the surface by ellipsometry, identify the presence of Si−OH groups by FTIR spectroscopy, and quantify the number density of surface radicals by the TEMPO binding assay, it is suggested that surface peroxides may be formed by hydrogen plasma treatment of silicon surfaces in the presence of adsorbed surface water.

AFM imaging of the silicon wafers demonstrated that the rms surface roughness of the native silicon wafer (R_{rms} = 0.17 nm) was essentially unaltered following surface hydrolysis and AP plasma treatment (R_{rms} = 0.20 nm) over a treatment period of 60 s. However, plasma treatment of the silicon substrate did result in increased surface hydrophilicity as indicated by the decrease in the water contact angle with increased plasma exposure period (Figure 7). It is noted, though, that at the optimal plasma activation exposure time for surface radical formation (treatment time 10 s) the contact angle of the plasma-treated surface decreased by only 13% relative to that of the untreated surface (i.e., from 61 to 53°).

Graft Polymerization. AP PIGP of 1-vinyl-2-pyrrolidone (VP) onto the silicon substrate (silicon-*g*-PVP) was initially conducted at the optimal surface plasma activation conditions (10 s plasma exposure period, rf power of 40 W, and 50% RH at 22 °C). The polymer-modified surfaces were characterized by atomic force microscopy with respect to surface feature number density and spacing, surface feature height distribution, rms surface roughness (R_{rms}, eq 1), and polymer volume. Also, it was noted that the contributions of small features to surface roughness may be

(59) Yoshida, W.; Castro, R. P.; Jou, J. D.; Cohen, Y. *Langmuir* **2001**, *17*, 5882−5888.

Table 1. Characteristics of PVP-Grafted Silicon in Aqueous Solvent as a Function of Initial Monomer Concentration

reaction condition[a]			
$[M]_0$ (% v/v)[a]	T (°C)	R_{rms} (nm)[b]	polymer volume ($nm^3/\mu m^2$)(10^3)[b]
10	80	0.177	5.9
20	80	0.317	25.0
30	80	0.412	52.3
40	80	0.468	37.9
50	80	0.365	24.8

[a] Surface initiation at a plasma treatment time of 10 s and rf power of 40 W. [b] Polymer surface feature properties determined by AFM.

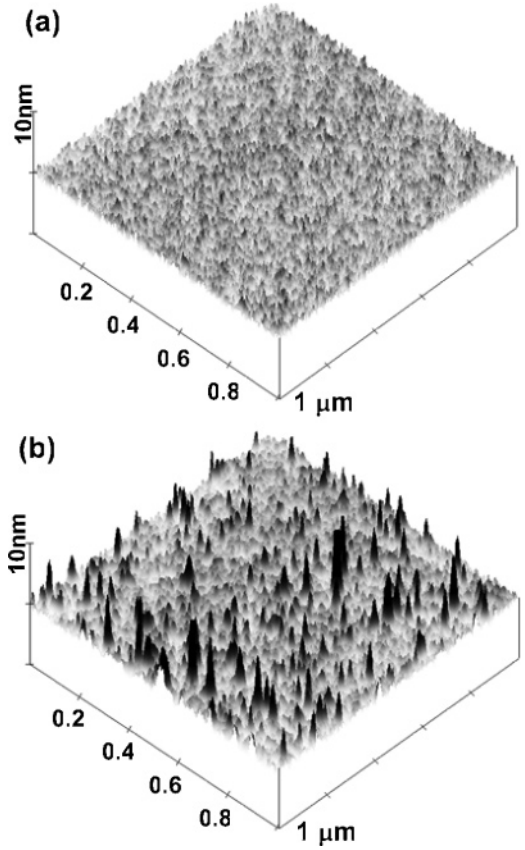

Figure 8. Tapping mode AFM surface images ($1 \times 1\ \mu m^2$) of (a) native silicon and (b) polymer-grafted silicon in aqueous solvent at $[M]_0 = 30\%$ (v/v) 1-vinyl-2-pyrrolidone at $T = 80$ °C.

eclipsed by a lower density of larger surface features.[11] Therefore, the distribution of polymer surface feature heights and skewness (S_{skew}, eq 2) were analyzed to provide a more descriptive topological surface characterization.

Graft polymerization was initially performed in an aqueous solvent, which is the most commonly used media for polymerization of VP.[9,31] Results of graft polymerization in an aqueous solvent (Table 1), where the initial monomer concentration was increased from $[M]_0 = 10-50\%$, revealed a grafted polymer volume that was maximized at about $[M]_0 = 30\%$, with nearly a factor of 9 increase in the polymer volume and an increase in surface roughness relative to $[M]_0 = 10\%$. Furthermore, the rms surface roughness ($R_{rms} = 0.412$ nm) of the surface grafted at $[M]_0 = 30\%$ was about a factor of 2.4 greater than the rms roughness of the native silicon wafer. As the initial monomer concentration was increased above 30%, the polymer volume decreased by more than 50% at $[M]_0 = 50\%$. Measurements of film thickness by ellipsometry were not feasible because of the low surface density of grafted polymers. Also, water contact angle measurements of PVP-grafted surfaces did not show a measurable change (<5%) in surface hydrophilicity because of the low surface coverage of grafted polymers. AFM imaging of the PVP-grafted silicon substrates created in the above aqueous graft polymerization step was used to reveal the topography of the modified surfaces (Figure 8). Although these studies were useful in identifying the optimal monomer concentration for grafting at $[M]_0 = 30\%$, AFM imaging suggested that the above grafting approach was not capable of producing high-density surface grafting, which may have been due, in part, to the aqueous solvent. Water contact angle measurements of the hydrolyzed surface (61°) suggested a low degree of hydrophilicity, indicating poor solvent−substrate surface wetting that may have been insufficient for graft polymerization in the aqueous solvent. *N*-Methyl-2-pyrrolidone (NMP), an organic solvent miscible in

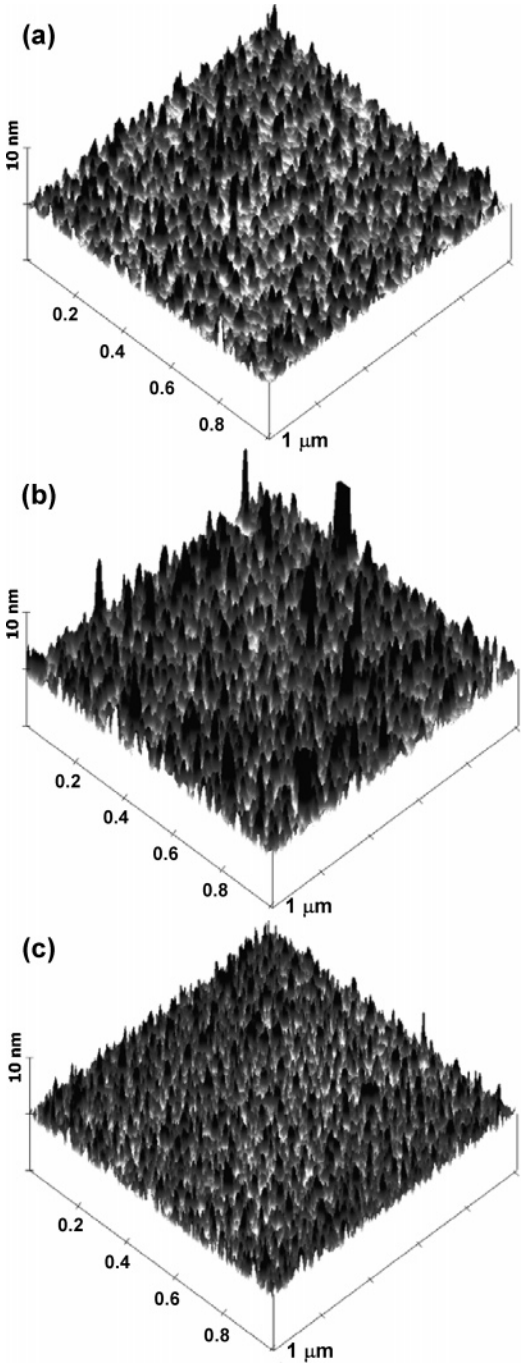

Figure 9. Tapping mode AFM surface images ($1 \times 1\ \mu m^2$) of polymer-grafted silicon in *N*-methyl-2-pyrrolidone solvent at $[M]_0$ = (a) 20, (b) 30, and (c) 40% (v/v).

Table 2. Characteristics of PVP-Grafted Silicon in *N*-Methyl-2-pyrrolidone Solvent as a Function of Initial Monomer Concentration

reaction condition[a]						
$[M]_0$ (% v/v)[a]	T (°C)	contact angle (deg)	R_{rm} (nm)[b]	PVP film thickness (nm)[c]	polymer volume ($nm^3/\mu m^2$, 10^3)[b]	feature spacing (nm)[b]
10	80	54	0.179	1.7	20.1	25−35
20	80	43	0.423	2.3	49.9	5−20
30	80	38	0.724	5.5	138.9	5−10
40	80	49	0.382	2.7	85.3	5−10
50	80	51	0.264	2.3	35.4	20−30

[a] Surface initiation at plasma treatment time = 10 s and rf power = 40 W. [b] Polymer surface feature properties determined by AFM. [c] PVP layer thickness measured by spectroscopic ellipsometry.

Table 3. Average Feature Diameter and Feature Spacing for PVP-Grafted Silicon in a Solvent Mixture of *N*-Methyl-2-pyrrolidone (NMP) in Water

reaction condition[a]			
[NMP] (% v/v)[a]	$[M]_0$ (% v/v)	av feature diameter (nm)[b]	feature spacing (nm)[b]
0	30	10.51	100−200
20	30	27.44	30−80
40	30	50.16	25−60
60	30	92.33	10−50
80	30	43.24	5−20
100	30	17.06	5−10

[a] Surface initiation at plasma treatment time = 10 s and rf power = 40 W. [b] Polymer surface feature properties determined by AFM.

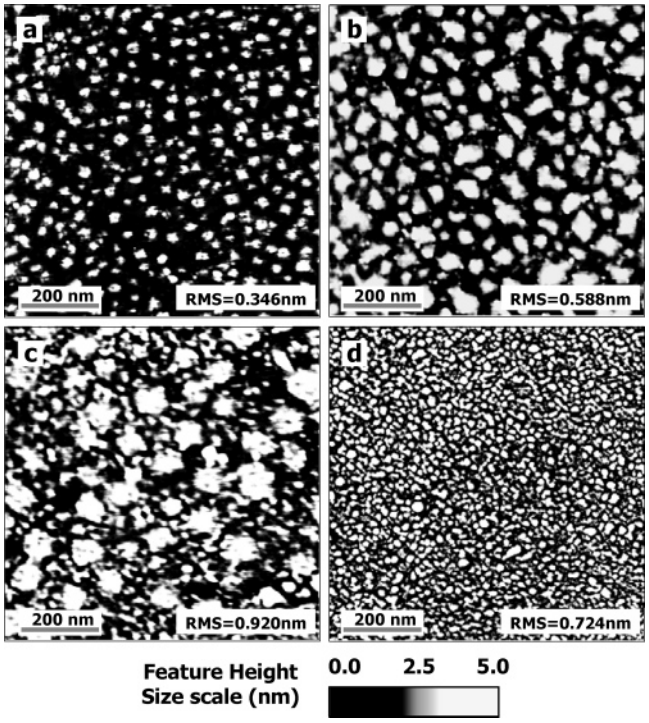

Figure 10. Tapping mode AFM images (1×1 μm^2) of polymer-grafted silicon at $[M]_0 = 30\%$ (v/v) in a mixture of aqueous solvent and (a) [NMP] = 15% (v/v), (b) [NMP] = 40% (v/v), (c) [NMP] = 60% (v/v), and (d) [NMP] = 100% (v/v) (no water).

both monomer and substrate, was chosen as a substitute for DI water for comparative purposes to improve the grafting density. Contact angle measurements with NMP as the wetting agent demonstrated that the native silicon surface was completely wetted (<5°) by the organic solvent.

Graft polymerization in NMP indeed resulted in a higher density of surface-grafted features as observed by AFM imaging (Figure 9), evidencing a higher density of polymer chains as compared to graft polymerization in an aqueous solvent. PVP-grafted surfaces obtained by graft polymerization in NMP demonstrated an increase in polymer volume with increasing initial monomer concentration (Table 2) up to a maximum obtained at $[M]_0 =$ 30%, which is qualitatively consistent with studies performed in aqueous solvent. Surfaces grafted at $[M]_0 = 30\%$ as compared to those grafted at $[M]_0 = 10\%$ demonstrated both a 3-fold increase in polymer layer thickness and a corresponding decrease of 30% in water contact angle. The increase in grafted layer thickness with increasing initial monomer concentration is consistent with previous work on the kinetics of free radical graft polymerization of 1-vinyl-2-pyrrolidone that conclusively demonstrated a rise in surface polymer graft yield with initial monomer concentration.[9] It was noted in the current study, however, that when the initial monomer concentration was increased to above 30% (i.e., 40 and 50% as given in Table 2) there was a decrease in the grafted polymer volume by 60 and 75%, respectively. It should be noted that whereas the polymer layer thickness obtained at $[M]_0 =$ 40% decreased by about 50%, relative to the maximum thickness attained at $[M]_0 = 30\%$, there was no apparent decrease in the surface graft density of polymer features. The increase in layer thickness with initial monomer concentration (at approximately $[M]_0 \leq 30\%$) is as expected given the higher rate of monomer addition to growing chains (i.e., propagation). However, chain termination (due to both chain transfer and chain−chain termination) also increases with monomer concentration. Therefore, one would expect that the film thickness will be reduced at high initial monomer concentrations as reported in Table 2. In principle and as verified by data up to the initial monomer concentration of 40%, chain surface density appeared to be affected primarily by the creation of active surface sites by the plasma treatment process. However, at sufficiently high monomer concentration, as observed in the present study for $[M]_0 = 50\%$, apparent feature spacing was reduced relative to $[M]_0 = 30$ and 40%. This unexpected result could be merely a reflection of the limitations of the AFM probing technique to recognize grafted polymer chains with feature heights of less than about 1 nm. A comparison of surfaces grafted in NMP solvent as opposed to an aqueous solvent demonstrated a striking difference in surface feature spacing. For example, for initial monomer concentration $[M]_0 = 30\%$, grafting in NMP solvent resulted in surface feature spacing of 5 to 10 nm as compared to a range of 100 to 200 nm when grafting in an aqueous solvent. Moreover, relative to aqueous studies, graft polymerization in NMP resulted in more than a 160% increase in grafted polymer volume, a 75% increase in surface roughness, and a significant increase in polymer graft density.

Given the prominent differences in the characteristics of the grafted polymer obtained by graft polymerization in NMP relative to that in an aqueous solvent, it was logical to assume that the surface morphology and polymer graft density could be uniquely tuned by adjusting the ratio of organic to aqueous media in the solvent mixture. Indeed, as shown in Table 3, the average polymer feature diameter increased by nearly a factor of 9 at [NMP] = 60% relative to pure aqueous solvent, and the feature spacing size decreased to a range of 10 to 50 nm, suggesting the formation of large close-proximity features on the surface. However, as the NMP/water ratio was further increased to [NMP] = 80%, the feature diameter decreased by more than 50%, and the feature spacing further decreased to a range of 5 to 20 nm, indicating the formation of a higher surface number density of smaller grafted polymer chains. AFM images illustrate these findings,

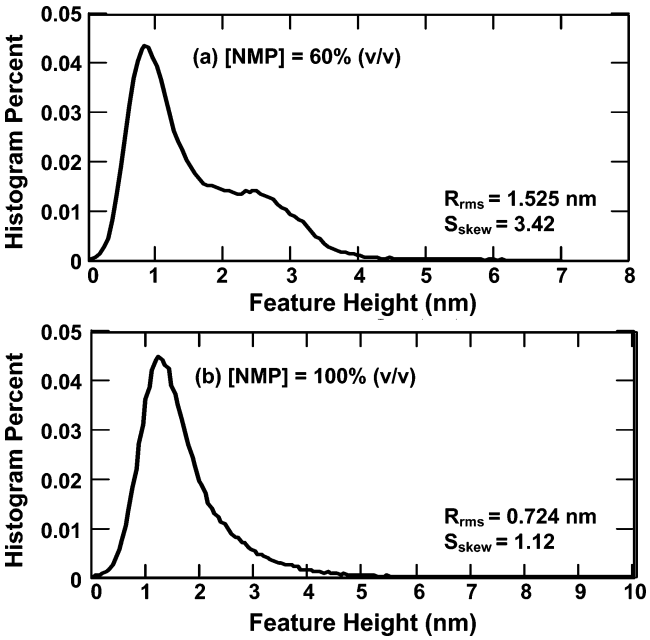

Figure 11. AFM height histograms of PVP-grafted silicon at $[M]_0$ = 30% (v/v) in a solvent composition of [NMP] = (a) 60 and (b) 100% (treatment time = 10 s, rf power = 40 W, and RH = 50% at 22 °C).

demonstrating that the grafted PVP layer that formed at [NMP] = 60% (Figure 10c) was composed of large clusters of grafted polymers compared to smaller grafted polymer features that resulted from grafting at [NMP] = 40% (Figure 10b) as well as at [NMP] = 15% (Figure 10a). For a low NMP/water mixture ratio, the modified surfaces were characterized by a homogeneous distribution of uniformly distributed surface features. As the NMP/water mixture ratio increased to [NMP] = 60%, a distinct mixture of small and large spherical polymer islands was formed, as noted by AFM imaging. Also, there was a significant increase in rms surface roughness from R_{rms} = 0.346 nm at [NMP] = 15% to R_{rms} = 0.920 nm at [NMP] = 60%. These findings suggest that the surface morphology of the grafted polymers can be tuned by altering the solvent−substrate wetting properties.

The effect of NMP on the topology of the high surface density (i.e., polymer feature spacing >50 nm) grafted polymer layers can be conveniently illustrated by inspecting the height histograms of the polymer surface features. As a comparison, the height histograms for the grafted PVP layers formed in NMP/water mixtures of [NMP] = 60 and 100% at $[M]_0$ = 30% are shown in Figure 11a,b, respectively. Whereas previous results showed an increased surface roughness for grafting at [NMP] = 60% (R_{rms} = 1.525 nm) compared to that at [NMP] = 100% (R_{rms} = 0.724 nm), the surface feature height histogram clearly reveals that the grafted polymer surface formed at [NMP] = 60% has a bimodal feature height distribution. This may be expected when considering the shape, morphology, and height of the polymer surface features imaged by AFM at [NMP] = 60% (Figure 10c) as compared to that at [NMP] = 100%. The bimodal distribution may be characterized by smaller features in the size range below 1 nm and larger clusters in the range of 1−8 nm (Figure 11a). Whereas smaller features contribute to the overall number density of surface features, larger features that appear as polymer clusters make a disproportionately large contribution to the rms surface roughness as a result of the increased diameter or surface area of the features (eq 1). It is hypothesized that the large polymer clusters or aggregates may have formed as the result of nonuniform surface wetting by the NMP/water mixture solvent. In contrast, grafting in pure NMP resulted in a continuous single-mode distribution of surface feature height with S_{skew} = 1.12 (Figure 11b) relative to S_{skew} = 3.42 for grafting at [NMP] = 60%. The above results demonstrate that 1-vinyl-2-pyrrolidone graft polymerization in pure NMP resulted in a narrower size distribution of tethered chains relative to the NMP/water mixtures. In closure, the present approach demonstrated that the topology of the grafted polymer layer could be controlled by the proper selection of reaction conditions and water/NMP mixture composition, thereby enabling a wide range of potential practical applications.[60]

Conclusions

Surface graft polymerization of 1-vinyl-2-pyrrolidone onto silicon was achieved by atmospheric pressure (AP) plasma surface initiation followed by free radical graft polymerization. The surface density of initiation sites was controlled by both the conditions of plasma generation (plasma gas, treatment time, and rf power) and adsorbed surface water. The grafted polymer layer exhibited significant differences in surface topology depending on the number density of surface-active sites generated by plasma treatment and polymerization conditions (solvent composition, initial monomer concentration, reaction temperature, and reaction time). Graft polymerization in a water/NMP solvent mixture resulted in a bimodal distribution of surface feature heights, presumably because of nonuniform surface wetting. Use of the above solvent mixture led to large polymer clusters with feature separation that decreased with the content of NMP in the solvent mixture. In contrast, graft polymerization in pure NMP resulted in grafted polymer surfaces with grafted chains of higher surface density and of greater size uniformity. Success with the present approach to surface graft polymerization suggests its potential use for large-scale surface nanostructuring with polymers.

Acknowledgment. This work was funded, in part, by the California Department of Water Resources and the U.S. Environmental Protection Agency.

LA700577P

(60) Cohen, Y.; Lewis, G. Graft Polymerization Induced by Atmospheric Pressure Plasma. U.S. Patent, Provisional Patent Application 60/857874, Nov 10, 2006.